DNA Structures

DOI: 10.1002/ange.201202677

A Molecular Translator that Acts by Binding-Induced DNA Strand Displacement for a Homogeneous Protein Assay**

*Feng Li, Hongquan Zhang, Chong Lai, Xing-Fang Li, and X. Chris Le**

Recent advances in DNA nanotechnology, including DNA nanostructures,[1] nanomachines,[2] logic gates,[3] and catalytic circuits,[4] have shown great potential as signal outputs for molecular imaging and disease diagnostics.[5] To achieve the detection of a specific target molecule with the DNA nanostructure, translation of the input target molecule into a unique output DNA to trigger the following assembly is one of the key steps.[5] Thus, many efforts have been directed to molecular translators based on nucleic acids.[5,6] For example, Ghadiri and co-workers have designed universal molecular translators that were able to convert any target nucleic acids to a predesigned output DNA for signal generation.[7] This approach was based on the previous discovery that DNA strand-exchange reactions can be accelerated by 10^6-fold using toehold-mediated strand displacement.[8] Turberfield and co-workers further showed the potential of "remote toehold" systems to be used as control for molecular translators.[9] By incorporating structure-switching aptamers to molecular translators, Liu and co-workers were able to use small molecules, for example, adenosine, to trigger changes in DNA structures.[10] However, applications of molecular translators have been limited to nucleic acids and a few small molecules. We aim to broaden the scope to include proteins.

Recent studies have shown that binding of two affinity ligands to the same target molecule was able to enhance the stability of DNA duplexes by increasing their local concentrations, thus resulting in binding-induced DNA assemblies.[11] We reason that the increased local concentration should be able to accelerate DNA strand-displacement reactions, which can potentially be applied to design a molecular translator for protein detection. We show herein a molecular translator that acts by binding-induced DNA strand displacement (abbreviated: binding-induced molecular translator) and demonstrate its application to an assay for proteins.

Our binding-induced molecular translator (Scheme 1) is composed of target-recognition and signal-output elements. Target recognition is achieved by two specific affinity ligands binding to the target protein. One affinity ligand is linked to DNA1 (blue in Scheme 1) and is conjugated to the gold nanoparticle (AuNP, 20 nm), which serves as the scaffold for the molecular translator. The second affinity ligand is conjugated to DNA2 (red), which serves as the competing DNA. An output DNA (DNA3, green) is initially hybridized to DNA1 to form a stable DNA1/DNA3 duplex. The three DNA sequences are designed in such a way that the complementary sequences between DNA1 and DNA3 are 2–4 nucleotides (n.t.) longer than the complementary sequences between DNA1 and DNA2. Thus, in the absence of the molecular target and the absence of affinity binding, displacement of output DNA3 by competing DNA2 is minimal. However, in the presence of the target molecule, the binding of the target molecule to the two affinity ligands that are

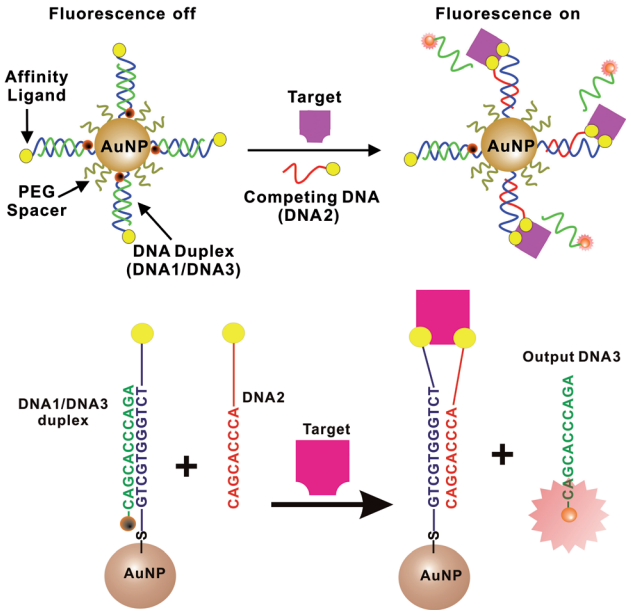

Scheme 1. Schematic illustration of the principle of the binding-induced molecular translator. The molecular translator is composed of a DNA1-functionalized gold nanoparticle scaffold (DNA1 is depicted in blue) and a competing DNA (DNA2, red); both DNA1 and DNA2 are conjugated to a specific affinity ligand for the target recognition. The fluorescently labeled output DNA3 (green) is initially hybridized to DNA1 on the AuNP, and thus its fluorescence is quenched by the AuNP. Binding of the two affinity ligands to the same target assembles DNA2 onto the AuNP scaffold, and thus triggers strand displacement between DNA2 and DNA3. Release of the output DNA3 from the duplex and from the AuNP scaffold results in a fluorescent signal. PEG = poly(ethylene glycol).

[*] F. Li, Prof. X. C. Le
Department of Chemistry, University of Alberta
Edmonton, T6G 2G3 (Canada)
E-mail: xc.le@ualberta.ca
Prof. H. Zhang, C. Lai, Prof. X.-F. Li, Prof. X. C. Le
Department of Laboratory Medicine and Pathology
University of Alberta
Edmonton, T6G 2G3 (Canada)

[**] We thank the Natural Sciences and Engineering Research Council of Canada, the Canadian Institutes of Health Research, the Canada Research Chairs Program, and Alberta Health and Wellness for financial support.

Supporting information for this article is available on the WWW under http://dx.doi.org/10.1002/anie.201202677.

linked to DNA1 and DNA2 brings DNA2 into close proximity to the DNA1/DNA3 duplex. This binding-induced assembly of DNA2 around the AuNP scaffold greatly increases the local concentration of DNA2 and accelerates the strand-displacement reaction between DNA2 and DNA3. As a consequence, the output DNA3 is released from the scaffold. The subsequent detection signal can be generated by directly monitoring the displaced output DNA3 or by using the output DNA to trigger further DNA assembly.

To test the feasibility of our strategy, we first designed a molecular translator for streptavidin by using biotin as the affinity ligand (Figure S1 in the Supporting Information). DNA1 and DNA2 are each conjugated to a biotin molecule. DNA3 is labeled with a fluorescent dye, tetramethylrhodamine, and the 11 n.t. sequence of DNA3 is complementary to DNA1. Hybridization of DNA3 to DNA1 results in fluorescence quenching of the dye by the AuNP. Thus, in the absence of streptavidin, the fluorescence of the system is "off". In the presence of streptavidin, binding of streptavidin to biotinylated DNA1 and DNA2 brings competing DNA2 onto the AuNP scaffold, thereby enhancing competition of DNA2 with DNA3. The binding-induced assembly increases the local concentration of DNA2 and accelerates the kinetics of the strand displacement. The displaced output DNA3 is released from the AuNP scaffold and the fluorescence is turned "on". By measuring the fluorescence signal from DNA3, we are able to assess the performance of the binding-induced molecular translator.

Figure 1 shows the fluorescence intensities of the output DNA3 as a result of the binding-induced molecular translation process. Fluorescence intensities from solutions containing streptavidin (10 nM) are readily distinguishable from the blank (Figure 1 A). The measured fluorescence intensities are proportional to the concentration of streptavidin in the range of 0.1–25 nM (Figure 1 B), thus providing a quantitative measure of the protein concentration.

To confirm that the binding-induced translation is a target-specific process, we tested our system using streptavidin (10 nM) that was fully saturated with biotin (500 μM; control 1 in Figure 1 A). The results are similar to those of the blank. Likewise, in the absence of the competing DNA2 (control 2 in Figure 1 A) the observed background fluorescence intensity is similar to that of the blank. These results suggest that specific binding is the triggering process for the successful binding-induced molecular translation.

A key concept to our success in the efficient molecular translation of a protein into a predesigned output DNA is the binding-induced DNA strand displacement that is accelerated upon target binding and minimized in the absence of target binding. Among others, the following factors play major roles in DNA displacement kinetics and can potentially alter the rate of the DNA strand-displacement reaction: the length of the DNA1/DNA3 duplex, the concentration and length of the competing DNA2, and the temperature.[12] Owing to the rational design, the primary driving force of the binding-induced strand-displacement reaction was the dramatic increase of the local concentration of the competing DNA upon the binding-induced DNA assembly.[11] We designed the DNA1/DNA3 duplex to have 11 base pair complementary

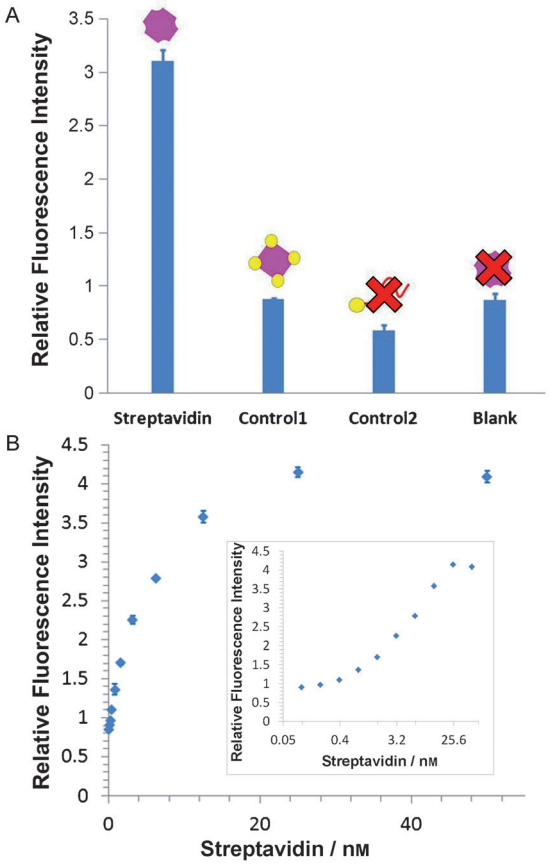

Figure 1. Evaluation of the binding-induced molecular translator for streptavidin using a fluorescent turn-on assay. A) The streptavidin test solution contained DNA1-AuNP conjugates (0.5 nM), competing DNA2 (40 nM), and streptavidin (10 nM). Control 1 contained the same amount of reagents as the streptavidin test solution except that the streptavidin binding sites were saturated with biotin (500 μM). Control 2 was carried out using the same concentrations of DNA1-AuNP conjugates and streptavidin, but no competing DNA2. In the blank, all reagents and probes were identical to the streptavidin test solution, but no streptavidin was added. B) Increases in relative fluorescence as a function of concentrations of streptavidin. The inset plot shows increases in relative fluorescence intensity as a function of streptavidin concentrations using a logarithmic scale.

sequences that have a melting temperature (T_m) of 40 °C at the experimental conditions. The selection of these DNA sequences was based on two considerations: 1) the melting temperature has to be high enough to ensure a stable DNA1/DNA3 duplex at room temperature; and 2) DNA3 can be displaced quickly by DNA2 upon the target binding.

The strand displacement can potentially be tuned by varying the length of the competing DNA2 (e.g., 7, 8, or 9 n.t. as shown in Figure S2 A in the Supporting Information). In principle, a shorter competing DNA2 sequence could reduce the nonspecific strand displacement. However, shorter competing DNA sequences also lead to lower specific signal intensities (Figure S2 in the Supporting Information). We chose a competing DNA2 that has 9 n.t. complementary to DNA1. The T_m value of the 9 n.t. DNA2/DNA1 duplex is 32.4 °C. Upon the target binding that assembles DNA2 and DNA1 to form a closed-loop and stem structure (Figure S1 in

the Supporting Information), the T_m value is increased to 56.4 °C. Thus, the dramatic increase in the stability of the closed-loop structure formed after affinity binding favors the binding-induced strand displacement over the target-independent (nonspecific) strand displacement.

To further reduce the nonspecific strand displacement, we introduced a blocking oligo (B10 to B12, for sequences see Figure S3 A in the Supporting Information) to partially hybridize with DNA2 (Figures S3 and S4 in the Supporting Information). The blocking oligo (10–12 n.t.) was designed to hybridize to a poly(T) sequence of 6–8 n.t. and 4 n.t. of the competing sequence of DNA2 (Figure S3 A in the Supporting Information). Hybridized to this blocking oligo, DNA2 is left with a competing sequence of only 5 n.t., thereby making it unfavorable to compete and displace DNA3 from the DNA1/DNA3 duplex. The duplex between the blocking oligo and DNA2 (estimated T_m 30.8 °C) can be stable under the annealing temperature of 25 °C. The use of a blocking oligo (e.g., B10) resulted in a reduction of background fluorescence without adversely affecting the fluorescence signal of the target (Figure S3B in the Supporting Information).

Because the kinetics of strand displacement are dependent on the temperature,[7] we have examined the effect of temperature on the performance of the binding-induced molecular translator (Figure S5 in the Supporting Information). The rate of the binding-induced strand-displacement process can be accelerated by increasing the incubation temperature (e.g., 37 °C) to be near the T_m value of the DNA1/DNA3 duplex. The influence of other parameters, for example, the ratio between AuNP concentration and competing DNA2 (Figure S6 in the Supporting Information) is shown in the Supporting Information.

The AuNP scaffold integrated in our binding-induced molecular translator serves two primary functions: 1) to quench the fluorescence of the hybridized DNA3 probe, and 2) to increase the local concentration of the assembled DNA in a small volume.[13] To demonstrate the general applicability of this strategy and to confirm the importance of increasing the local concentrations, we designed three molecular translators for a clinically relevant protein, the platelet-derived growth factor BB (PDGF BB). An aptamer was used as the affinity ligand to bind to PDGF BB. The molecular translator in design 1 (Figure 2 A) was constructed in the same way as for the streptavidin–biotin system. Both DNA1 and DNA2 were extended by including a 44 n.t. PDGF aptamer (Table S2 in the Supporting Information). The extended DNA1 was then conjugated to the AuNP and hybridized with DNA3. Thus binding of PDGF BB to two aptamers resulted in the binding-induced strand displacement of DNA3. Detection of the displaced DNA3 showed a quantitative relationship between the fluorescence and the concentrations of PDGF BB (red curve in Figure 2 D).

We further examined the influence of the density of the DNA1/DNA3 duplex on the AuNP (Figure S7 in the Supporting Information). The observed increases in fluorescence intensity with the increase of DNA density on the AuNP are consistent with the role of the increased local concentration on the performance of the binding-induced molecular translator.

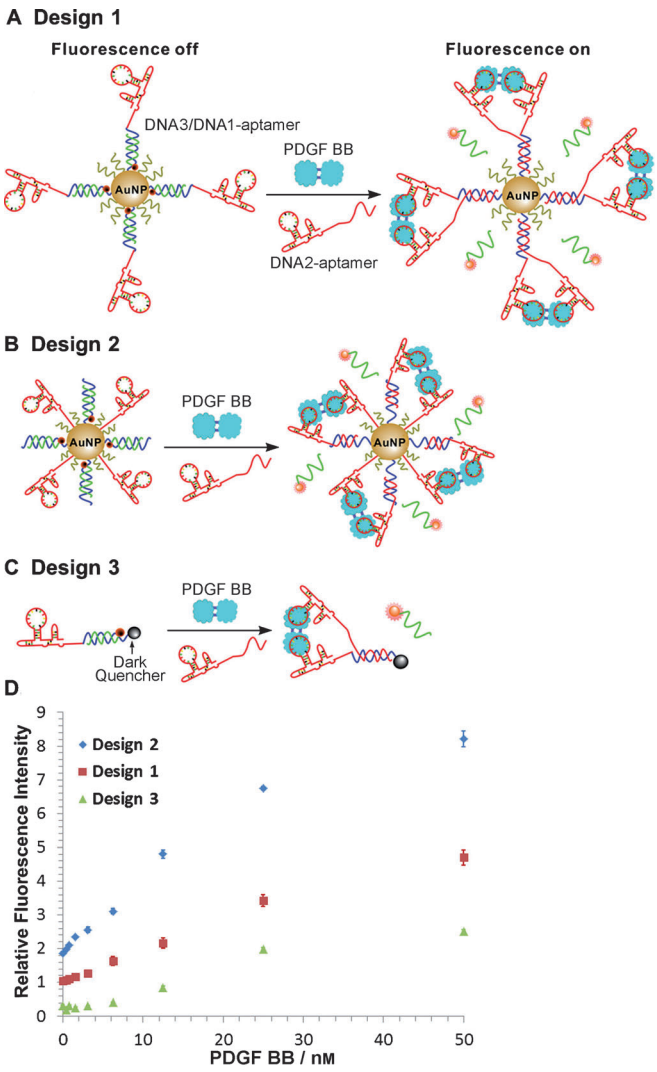

Figure 2. A–C) Schematic illustrations of three design strategies to construct the molecular translators for PDGF BB. D) Performance of the three molecular translator designs, as assessed by detecting PDGF BB (0–50 nM). The total concentration of the fluorescently labeled output DNA was kept at 40 nM for all samples.

In design 2 (Figure 2 B, Figure S8 in the Supporting Information), the PDGF aptamer and DNA1 were each directly conjugated to the AuNP, at an equal ratio. The AuNP served as a scaffold to facilitate binding of PDGF BB to two aptamers and the binding-induced strand displacement. As compared to design 1, DNA1 in design 2 was not extended with a 44 n.t. aptamer. Therefore, the volume of the DNA1-functionalized AuNP in design 2 is smaller than in design 1. A higher local concentration is expected for the binding-induced assembly in a smaller volume. The results from testing PDGF BB using design 2 indeed showed higher signal intensities than those obtained using design 1 (Figure 2 D).

As a comparison, we also constructed a third molecular translator using a dark quencher instead of a AuNP (Figure 2 C). The fluorescence of the output DNA was as much as fourfold lower than of the other two designs (Figure 2 D). These results are consistent with the notion that the local

concentrations of the DNA assembly are substantially increased on the AuNP scaffold.

In conclusion, we have successfully constructed a binding-induced molecular translator that is able to convert the input protein information to readily detectable output DNA. Binding of the specific protein to affinity ligands on both the output DNA duplex and the competing DNA assembled them on the AuNP scaffold and lead to increased local concentrations, thereby resulting in binding-induced strand displacement. The displaced output DNA was easily detectable with fluorescent dyes as labels. Other molecular translator formats, for example, catalytic DNA circuits, could be achieved by incorporating functional DNA domains instead of fluorescent dyes in the output DNA and by using the principle of toehold-mediated strand displacement. Furthermore, many proteins can bind to two affinity probes and are amenable to sandwich assays (e.g., enzyme-linked immunosorbent assays (ELISAs)). Thus, the concept and strategy reported herein can also be applied to construct binding-induced molecular translators for these and other molecular targets to which two or more affinity probes can bind. Potential applications range from assays for specific molecular targets, to imaging and point-of-care diagnostics, and binding-induced nanodevices.

Received: April 6, 2012
Revised: July 23, 2012
Published online: August 15, 2012

Keywords: DNA assembly · DNA structures · molecular translator · proteins · strand displacement

[1] a) E. Winfree, F. Liu, L. A. Wenzler, N. C. Seeman, *Nature* **1998**, *394*, 539 – 544; b) F. A. Aldaye, A. L. Palmer, H. F. Sleiman, *Science* **2008**, *321*, 1795 – 1799; c) S. M. Douglas, H. Dietz, T. Liedl, B. Hogberg, F. Graf, W. M. Shih, *Nature* **2009**, *459*, 414 – 418.

[2] a) J. Bath, A. J. Turberfield, *Nat. Nanotechnol.* **2007**, *2*, 275 – 284; b) S. Modi, G. S. M. D. Goswami, G. D. Gupta, S. Mayor, Y. Krishnan, *Nat. Nanotechnol.* **2009**, *4*, 325 – 330; c) D. Y. Zhang, G. Seelig, *Nat. Chem.* **2011**, *3*, 103 – 113.

[3] a) G. Seelig, D. Soloveichik, D. Y. Zhang, E. Winfree, *Science* **2006**, *314*, 1585 – 1588; b) B. M. Frezza, S. L. Cockroft, M. R. Ghadiri, *J. Am. Chem. Soc.* **2007**, *129*, 14875 – 14879; c) L. Qian, E. Winfree, *Science* **2011**, *332*, 1196 – 1201.

[4] a) P. Yin, H. M. T. Choi, C. R. Calvert, N. A. Pierce, *Nature* **2008**, *451*, 318 – 323; b) G. Seelig, B. Yurke, E. Winfree, *J. Am. Chem. Soc.* **2006**, *128*, 12211 – 12220; c) R. M. Dirks, N. A. Pierce, *Proc. Natl. Acad. Sci. USA* **2004**, *101*, 15275 – 15278.

[5] a) B. Li, A. D. Ellington, X. Chen, *Nucleic Acids Res.* **2011**, *39*, e110; b) D. S. Seferos, D. A. Giljohann, H. D. Hill, A. E. Prigodich, C. A. Mirkin, *J. Am. Chem. Soc.* **2007**, *129*, 15477 – 15479; c) D. Zheng, D. S. Seferos, D. A. Giljohann, P. C. Patel, C. A. Mirkin, *Nano Lett.* **2009**, *9*, 3258 – 3261.

[6] a) S. Liao, N. C. Seeman, *Science* **2004**, *306*, 2072 – 2074; b) J. J. Tabor, M. Levy, A. D. Ellington, *Nucleic Acids Res.* **2006**, *34*, 2166 – 2172; c) A. V. Garibotti, S. Liao, N. C. Seeman, *Nano Lett.* **2007**, *7*, 480 – 483; d) M. Endo, S. Uegaki, T. Majima, *Chem. Commun.* **2005**, 3153 – 3155; e) S. Beyer, F. C. Simmel, *Nucleic Acids Res.* **2006**, *34*, 1581 – 1587.

[7] J. M. Picuri, B. M. Frezza, M. R. Ghadiri, *J. Am. Chem. Soc.* **2009**, *131*, 9368 – 9377.

[8] D. Y. Zhang, E. Winfree, *J. Am. Chem. Soc.* **2009**, *131*, 17303 – 17314.

[9] A. J. Genot, D. Y. Zhang, J. Bath, A. J. Turberfield, *J. Am. Chem. Soc.* **2011**, *133*, 2177 – 2182.

[10] Y. Xing, Z. Yang, D. Liu, *Angew. Chem.* **2011**, *123*, 12140 – 12142; *Angew. Chem. Int. Ed.* **2011**, *50*, 11934 – 11936.

[11] a) H. Yang, A. Z. Rys, C. K. McLaughlin, H. F. Sleiman, *Angew. Chem.* **2009**, *121*, 10103 – 10107; *Angew. Chem. Int. Ed.* **2009**, *48*, 9919 – 9923; b) H. Zhang, X.-F. Li, X. C. Le, *Anal. Chem.* **2012**, *84*, 877 – 884; c) Y. Sun, H. Liu, L. Xu, L. Wang, Q.-H. Fan, D. Liu, *Langmuir* **2010**, *26*, 12496 – 12499; d) C. Zhou, Z. Yang, D. Liu, *J. Am. Chem. Soc.* **2012**, *134*, 1416 – 1418.

[12] L. P. Reynaldo, A. V. Vologodskii, B. P. Neri, *J. Mol. Biol.* **2000**, *297*, 511 – 520.

[13] a) A. K. Lytton-Jean, C. A. Mirkin, *J. Am. Chem. Soc.* **2005**, *127*, 12754 – 12755; b) Y. F. Huang, H. T. Chuang, W. Tan, *Anal. Chem.* **2008**, *80*, 567 – 572; c) T. Zhao, Z. Yang, D. Liu, *Nanoscale* **2011**, *3*, 4015 – 4021; d) W. Wang, H. Liu, D. Liu, Y. Xu, Y. Yang, D. Zhou, *Langmuir* **2007**, *23*, 11956 – 11959.

